Anal. Chem. **1999,** *71,* 4649−4656

A Study of Depletion Layer Effects on Equivalent Circuit Parameters Using an Electrochemical Quartz Crystal Impedance System

Qingji Xie,* Jin Wang, Anhong Zhou, Youyu Zhang, Hongwei Liu, Zhinian Xu, Yu Yuan, Maoying Deng, and Shouzhuo Yao

Chemical Research Institute, Hunan Normal University, Changsha 410081, P.R. China

An electrochemical quartz crystal impedance system (EQCIS) was used to investigate depletion layer effects on equivalent circuit parameters of piezoelectric quartz crystal resonance in electrochemical processes of $CoSO_4$ aqueous solutions containing 0.4 mol/L ethylenediamine + 0.5 mol/L Na_2SO_4, 0.2 mol/L 1,10-phenanthroline + 0.5 mol/L Na_2SO_4 and $K_3Fe(CN)_6$, or $K_4Fe(CN)_6$ aqueous solutions containing 1.0 mol/L KCl in potential cycling experiments, respectively. The impedance data were analyzed according to Martin's model. For the former two systems, motional resistance R_1, series resonant frequency f_s, and motional inductance L_1 changed reversibly with potential, and the observed values of ΔR_1, ΔL_1, and Δf_s roughly satisfied equations reflecting liquid loading effects, suggesting that changes in these parameters might be mainly governed by local variations in solution density and viscosity near the electrode surface. For the latter two systems, reversible changes in R_1 with potential coincided well with the simulated results from variations in solution density and viscosity near the electrode surface; however, besides reversible changes of ΔL_1 and Δf_s with potential, rising drifts of f_s and decreasing drifts of L_1 were found at oxidation potentials. The drifts of f_s and L_1 observed are believed to result from mass changes of the gold electrode, and cyanide and chloride corrosion of the gold electrode at oxidation potentials may play an important role for the drifting phenomena. It is concluded that quantitative analyses of ΔR_1, ΔL_1, and Δf_s obtained from the EQCIS provide the possibility for differentiating the net depletion layer effect with the change in electrode mass, and the ΔR_1 response may be well used for evaluating local changes in liquid loading inside the depletion layer compared with responses of Δf_s and ΔL_1.

The electrochemical quartz crystal microbalance (EQCM) has been widely used in electrochemical studies owing to its in situ response to changes in mass loading on the electrode surface down to the monolayer or submonolayer level.[1−3] While much EQCM research concentrated on dc electrochemical modulations in combination with the quartz crystal microbalance (QCM) measurement, ac electrogravimetry was developed by Gabrielli and Keddam et al. through the use of a QCM in an ac regime combined with electrochemical impedance measurement.[4] In addition, Lee et al. pioneered meaningful research on depletion layer effects on EQCM responses during the electrochemical processes of $K_3Fe(CN)_6$ and $K_4Fe(CN)_6$ aqueous solutions containing 1.0 mol/L Na_2SO_4 and suggested that analysis of small values of frequency shift obtained from EQCM needs to account for changes in solution density and viscosity within the depletion layer.[5] However, a lot of factors are known to affect the oscillating frequency of EQCM significantly,[6−10] e.g., the design of the oscillating circuit, electrode mass, electrode surface roughness, viscosity, and density of the media in which the piezoelectric quartz crystal (PQC) is placed, indicating the impossibility of differentiating changes in the electrode mass from other factors including liquid properties when only the oscillating frequency is monitored.[9]

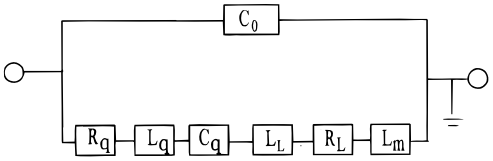

Figure 1. A modified Butterworth−Van Dyke equivalent electrical circuit for quartz crystal resonance. Where R_q, L_q, and C_q are motional resistance, motional inductance, and motional capacitance of the unperturbed crystal, respectively, R_L and L_L are the motional resistance and motional inductance due to liquid loading, respectively, L_m is the motional inductance due to mass loading, and C_0 is the static capacitance (note the parasitic capacitance in the test fixture that is introduced during admittance measurement[9] is not shown here).

Quartz crystal impedance analysis is an excellent method for investigating the PQC resonance. Martin et al.[9] reported a series of equations of equivalent circuit parameters and a modified

(1) Bruckenstein, S.; Shay, M. *Electrochim. Acta* **1985**, *30*, 1295.
(2) Buttry, D. A. In *Electroanalytical Chemistry*; Bard, A. J., Ed.; Marcel Dekker: New York, 1990; Vol. 17.
(3) Buttry, D. A.; Ward, M. D. *Chem. Rev.* **1992**, *92*, 1355.
(4) Gabrielli, C.; Keddam, M.; Nadi, N.; Perrot, H. *Electrochim. Acta* **1999**, *44*, 2095 and references therein.
(5) Lee, W.; White, H. S.; Ward, M. D. *Anal. Chem.* **1993**, *65*, 3232.
(6) Thompson, M.; Kipling, A. L.; Duncan-Hewitt, W. C.; Rajakovic, L. V.; Cavic-Vlasak, B. A. *Analyst* **1991**, *116*, 881.
(7) Kanazawa, K. K.; Gordon, J. G. *Anal. Chim. Acta* **1985**, *175*, 99.
(8) Schumacher, R.; Gordon, J. G.; Melroy, O. *J. Electroanal. Chem.* **1987**, *216*, 127.
(9) Martin, S. J.; Granstaff, V. E.; Frye, G. C. *Anal. Chem.* **1991**, *63*, 2272.
(10) Muramatsu, H.; Tamiya, E.; Karube, I. *Anal. Chem.* **1988**, *60*, 2142.

10.1021/ac981390z CCC: $18.00
Published on Web 09/18/1999

Butterworth−Van Dyke (BVD) equivalent electrical circuit as shown in Figure 1 for the characterization of a QCM with simultaneous mass and liquid loading. Their equations reflecting liquid loading effects can be expressed as[5,7,9]

$$\Delta f_{sL} = -\frac{f_{sg}^{3/2}}{(\pi\rho_q\mu_q)^{1/2}}[(\rho_{L2}\eta_{L2})^{1/2} - (\rho_{L1}\eta_{L1})^{1/2}] \quad (1)$$

$$\Delta R_L = \frac{4f_{sg}L_q(\pi f)^{1/2}}{(\bar{c}_{66}\rho_q)^{1/2}}[(\rho_{L2}\eta_{L2})^{1/2} - (\rho_{L1}\eta_{L1})^{1/2}] \quad (2)$$

$$\Delta L_L = \frac{2f_{sg}L_q}{(\pi f\,\bar{c}_{66}\rho_q)^{1/2}}[(\rho_{L2}\eta_{L2})^{1/2} - (\rho_{L1}\eta_{L1})^{1/2}] \quad (3)$$

where Δf_{sL}, ΔR_L, and ΔL_L are changes in series resonant frequency, motional resistance, and motional inductance due to variations of solution density ρ_L and viscosity η_L, respectively, f_{sg} is the series resonant frequency in air, ρ_q is the density of quartz (2648 kg m^{-3}), μ_q is the shear modulus for AT-cut quartz (2.947×10^{10} N/m^2), L_q is the motional inductance of the quartz crystal in air, $\bar{c}_{66}$ is the lossy piezoelectrically stiffened quartz elastic constant (2.957×10^{10} N/m^2),[11] and the subscripts of L1 and L2 denote the ρ_L and η_L of state 1 and state 2, respectively.

Some researchers have applied the modified BVD model to analyze quartz crystal impedance data obtained in situ during electrochemical processes; for example, Noël and Topart reported quartz crystal impedance measurements during metal and polypyrrole depositions,[11,12] Bandey et al. conducted dynamic quartz crystal impedance measurements of poly(vinylferrocene) film deposition,[13] Skompska and Hillman investigated the electropolymerization, electroactivity, and complexing properties of poly(1,8-diaminonaphthalene) films,[14] Ethenique, Calvo, et al. conducted electrochemical quartz crystal impedance studies of redox hydrogels with a fast transfer technique and indicated that with their setup one can acquire a complete transfer spectrum (50 kHz and 100 points) at a time interval of 10 ms.[15−17]

In this work, we aim at depletion layer effects of electrochemical processes on equivalent circuit parameters with use of an electrochemical quartz crystal impedance system (EQCIS), since a spatially nonuniform solution was seldom studied by EQCIS and multiple information obtained from the EQCIS may provide the possibility of differentiating responses to the net depletion layer effect and to mass change in electrochemical processes.

EXPERIMENTAL SECTION

Instrumentation and Chemicals. The EQCIS used included an HP 4395A network/spectrum/impedance analyzer, an EG&G M283 potentiostat, and two IBM personal computers with Intel cards for data sharing. Conductance G and susceptance B of piezoelectric quartz crystal resonance were measured synchronously on the HP 4395A equipped with an HP 43961A impedance test adapter and an HP 16092A test fixture. A user program was written in Visual Basic (VB) 5.0 to control the HP 4395A and to acquire admittance data via an HP 82341C high-performance HP-IB interface card for Windows 3.1/NT/95. A nonlinear least-squares fitting program based on the Gauss−Newton or Gauss−Newton−Marquardt algorithm was written in VB 5.0 for the simultaneous fits of G and B data after experiments.

AT-Cut 9- and 5-MHz piezoelectric quartz crystals (12.5 mm in diameter) were used in the experiments (the 5-MHz crystal was only used for the experiment shown in Figure 5). The silver electrode of 6.0-mm diameter was placed in air and connected to the nonground terminal of the HP 16092A impedance test fixture. The gold electrode of 6.5-mm diameter, vacuum-evaporated by using an Eiko IB-3 ion coater and a highly pure gold foil purchased from Hitachi Inc., was immersed in the test solution, connected to the ground terminal of the HP 16092A, and served as the working electrode too. The gold electrode had a surface polished to ∼0.1 μm as examined by a SEM. A saturated KCl calomel electrode (SCE) with a supporting electrolyte salt bridge served as the reference and all potentials in this work are referenced to it. A large-area platinum plate was used as the counter electrode. A capacitance of 220 μF was used to isolate the potentiostat from the HP 4395A. This isolation capacitance did not have significant influence on the crystal impedance measurements due to its much larger value than the static capacitance,[11] and more importantly, its effect was eliminated further during the compensation of the HP16092A impedance test fixture at the short compensation stage.

The surface of the gold electrode was treated generally by washing with 1 mol/L HNO_3 for 10 s and then scanned between 0 and −0.8 V vs SCE in 0.1 mol/L H_2SO_4 at 50 mV/s for at least five cycles. No detectable currents of impurities could be found. Other surface treatment approaches were also tested; e.g., the gold surface layer was dissolved in 1.0 mol/L KCl by switching the potential to 0.8 V to produce a fresh gold surface. We found that different surface treatment routines made no significant changes in EQCIS responses. All chemicals were analytical grade or better. $K_3Fe(CN)_6$ or $K_4Fe(CN)_6$ were twice recrystallized via pure water before use. Doubly distilled water and freshly prepared solutions were used throughout. The test solutions were deareated by passing a stream of pure nitrogen for at least 20 min prior to experiments.

The density values of various concentrations of $K_3Fe(CN)_6$ and $K_4Fe(CN)_6$ aqueous solutions containing 1.0 mol/L KCl were measured gravimetrically, and their viscosity values were determined relative to pure water by using an Ubbelohde viscometer of a capillary 0.6-mm inner diameter. We obtained linear relationships between the concentration of $K_3Fe(CN)_6$ or $K_4Fe(CN)_6$ (in mol/m^3) and solution density (in kg/m^3) or viscosity (in Pa s) as follows for concentrations smaller than 100 mmol/L:

$$\rho_{K_3Fe(CN)_6} = 0.1136C_{K_3Fe(CN)_6} + 1.039 \times 10^3 \quad (r = 0.9984) \quad (4a)$$

$$\rho_{K_4Fe(CN)_6} = 0.2213C_{K_4Fe(CN)_6} + 1.039 \times 10^3 \quad (r = 0.9996) \quad (4b)$$

(11) Noël, M. A.; Topart, P. A. *Anal. Chem.* **1994**, *66*, 484.
(12) Topart, P. A.; Noël, M. A. *Anal. Chem.* **1994**, *66*, 2926.
(13) Bandey, H. L.; Gonsalves, M.; Hillman, A. R.; Glidle, A.; Bruckenstein, S. *J. Electroanal. Chem.* **1996**, *410*, 219.
(14) Skompska, M.; Hillman, A. R. *J. Chem. Soc., Faraday Trans.* **1996**, *92*, 4101.
(15) Calvo, E. J.; Danilowicz, C.; Etchenique, R. *J. Chem. Soc. Faraday Trans.* **1995**, *91*, 4083.
(16) Calvo, E. J.; Etchenique, R.; Bartlett, P. N.; Singhal, K.; Santamaria, C. *Faraday Discuss.* **1997**, *107*, 141.
(17) Etchenique, R.; Calvo, E. J. *Anal. Chem.* **1997**, *69*, 4833.

$$\eta_{K_3Fe(CN)_6} = 1.676 \times 10^{-7} C_{K_3Fe(CN)_6} + 7.6644 \times 10^{-4} \quad (r = 0.9976) \quad (4c)$$

$$\eta_{K_4Fe(CN)_6} = 3.693 \times 10^{-7} C_{K_4Fe(CN)_6} + 7.6644 \times 10^{-4} \quad (r = 0.9996) \quad (4d)$$

Measurements of density and viscosity of the solutions containing $CoSO_4$ were not performed in this work, since $Co_2(SO_4)_3 \cdot 18H_2O$ as a strong oxidizing reagent ($E° = 1.83$ V) can be easily decomposed by water or moisture with evolution of oxygen[18] and thus was not commercially available.

Procedures. All G and B data were measured synchronously under conditions of 201 points, a frequency span of 30 kHz covering crystal resonant frequency, IF BW of 3 kHz, and source power of 0.5 dBm. Under such conditions, the HP 4395A completed one frequency scan within the given domain in 440.3 ms, and the computer was able to acquire G and B data at a frequency of 0.28 Hz. Prior to admittance measurements, the HP 43961A impedance test adapter and the HP 16092A test fixture were calibrated and compensated with use of HP standard impedance kits, respectively. The short compensation was conducted by using two identical leads in connection with the isolation capacitance to those for the crystal electrodes. G and B as functions of frequency were recorded simultaneously in electrochemical experiments. The G and B data were transferred into the nonlinear fitting program after the experiment for computing equivalent electrical parameters, by which one could also monitor experimental and fitted conductance and susceptance spectra in two VB 5.0 picture boxes, respectively.

Nonlinear Fitting of Admittance Spectra. Admittance Y, conductance G, and susceptance B for the modified Butterworth−Van Dyke equivalent electrical circuit as shown in Figure 1 can be expressed as[9,10]

$$Y = G + jB = \frac{R_1}{R_1^2 + U^2} + j\left(\omega C_0 - \frac{U}{R_1^2 + U^2}\right) \quad (5)$$

where $R_1 = R_q + R_L$, $\omega = 2\pi f$, $U = \omega L_1 - 1/(\omega C_q) = (1/C_q)(\omega/\omega_s^2 - 1/\omega)$, $L_1 = L_q + L_L + L_m$, and $\omega_s = 2\pi f_s$.

If the series resonant frequency f_s is defined as the frequency at which the motional reactance vanishes,[9,15,19] one obtains

$$\omega_s = 2\pi f_s = 1/(L_1 C_q)^{1/2} = 1/[(L_q + L_L + L_m)C_q)]^{1/2} \quad (6)$$

We measured G and B synchronously in experiments; therefore, G and B data acquired in one frequency scan were fitted simultaneously by using the above-mentioned nonlinear least-squares fitting program. R_1, C_0, $1/C_q$, and f_s were selected as estimation parameters during fitting. Typical values of equivalent circuit parameters obtained in air were about $R_q = 14.9\ \Omega$, $L_q = 7.86$ mH, $C_q = 40.2$ fF, and $C_0 = 12.3$ pF for 9-MHz crystals and about $R_q = 70.0\ \Omega$, $L_q = 43.62$ mH, $C_q = 23.4$ fF, and $C_0 = 11.4$ pF for 5-MHz crystals, respectively. The C_q values obtained are close to those calculated from Martin's equations,[9,11] i.e., 39.02 fF for a 9-MHz crystal and 22.31 fF for a 5-MHz crystal, respectively. The frequency giving maximum G, G_{max}, was automatically found by the program and used as the initial value of f_s, and $1/G_{max}$ was used as the initial value of R_1 during fitting iterations. The fitting iterations could be complete within ~3 s for a group of G and B data, when the sum of the residual square, q, and the relative sum of the residual square, q_r, as given in eq 7, had become minimum. Values of q_r obtained after fitting were generally between 5×10^{-6} and 1.4×10^{-5} for different 9-MHz crystals, which were so small that one could almost not see difference between the fitted and experimental admittance spectra by the naked eye. Values of q_r were randomly distributed at various potentials during one EQCIS experiment.

$$q_r = \frac{\sum_1^N (G_{fit} - G_{exp})^2 + \sum_1^N (B_{fit} - B_{exp})^2}{\sum_1^N G_{exp}^2 + \sum_1^N B_{exp}^2} = \frac{q}{\sum_1^N G_{exp}^2 + \sum_1^N B_{exp}^2} \quad (7)$$

where the subscripts, fit and exp, denote fitted and experimental results and N is the number of frequency points in experiments.

Calculation and Simulation of ΔR_L, Δf_{sL}, and ΔL_L Responses. Combination of eqs 1−3 yields

$$\Delta R_L = 2\pi f \Delta L_L = -\frac{4\pi L_q \Delta f_{sL} \sqrt{f\mu_q}}{\sqrt{\bar{c}_{66} f_{sg}}} \quad (8)$$

and typical values of the slope of ΔR_L vs Δf_{sL} are $-0.0986\ \Omega$/Hz for a 9-MHz crystal and $-0.547\ \Omega$/Hz for a 5-MHz crystal, respectively.

Accordingly, if experimental responses of ΔR_1, Δf_s, and ΔL_1 satisfy the following equation

$$\Delta R_1 = 2\pi f \Delta L_1 = -\frac{4\pi L_q \Delta f_s \sqrt{f\mu_q}}{\sqrt{\bar{c}_{66} f_{sg}}} \quad (9)$$

ΔR_1, Δf_s, and ΔL_1 should be completely governed by variations of solution density and viscosity near the electrode surface, i.e., a net depletion layer effect, otherwise, other factors such as mass changes may be effective besides the depletion layer effect.

Equations 1−3 and 8 are based on the assumption that ρ_L and η_L are constant throughout the solution, but this is not the case in an electrochemical experiment as both ρ_L and η_L are functions of the distance away from the electrode surface. Since in water the amplitude of the shear wave of a 5-MHz quartz crystal will decrease to $1/e$ of its original amplitude at a distance of 0.25 μm away from the crystal electrode surface,[5,7] the present work encounters the case of a nonuniform solution inside the depletion

(18) Nicholis, D. In *Comprehensive Inorganic Chemistry*; Bailar, J. C., Emeléus, H. J., Nyholm, S. R., Trotman-Dickenson, A. F., Eds.; Pergamon: New York, 1973; Vol. 3, Chapter 41.

(19) Martin, S. J.; Spates, J. J.; Wessendorf, K. O.; Schneider, T. W.; Huber, R. J. *Anal. Chem.* **1997**, *69*, 2050.

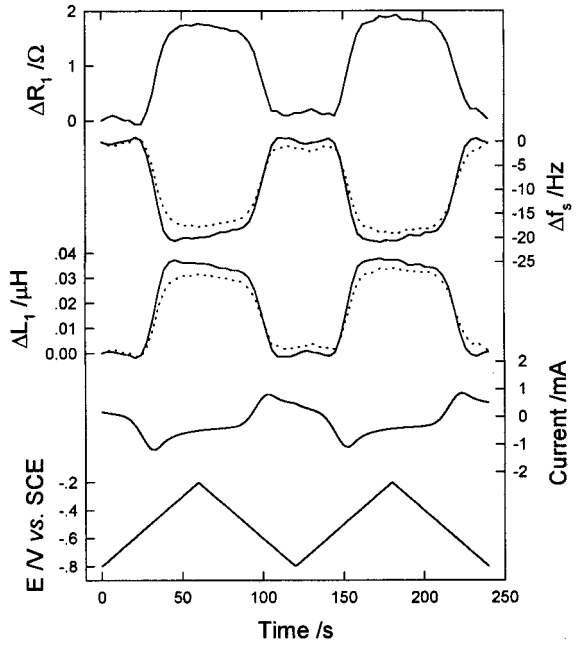

Figure 2. Simultaneous responses of current, ΔR_1, Δf_s, and ΔL_1 to potential cycling for a 9-MHz crystal in 60.0 mmol/L $CoSO_4$ aqueous solution containing 0.4 mol/L ethylenediamine + 0.5 mol/L Na_2SO_4. dE/dt = 10 mV/s. Solid lines, experimental; dashed lines, calculated according to eq 8 by assuming $\Delta R_L = \Delta R_1$.

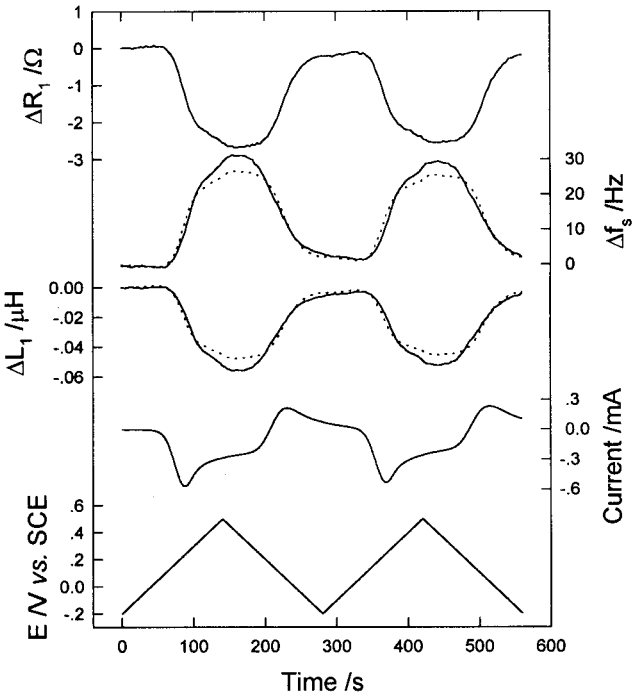

Figure 3. Simultaneous responses of current, ΔR_1, Δf_s, and ΔL_1 to potential cycling for a 9-MHz crystal in 50.0 mmol/L $CoSO_4$ aqueous solution containing 0.2 mol/L 1,10-phenanthroline + 0.5 mol/L Na_2SO_4. dE/dt = 5 mV/s. Solid lines, experimental; dashed lines, calculated according to eq 8 by assuming $\Delta R_L = \Delta R_1$.

layer. Local changes in the value of $(\rho_L \eta_L)^{1/2}$ near the electrode surface were estimated on the basis of eqs 15 and 16 in Lee's paper[5] and the assumption that values of ρ_L and η_L of the mixed solutions can be described as the linear combinations of the values of ρ and η (eq 4) of individual solutions of $K_3Fe(CN)_6$ and $K_4Fe(CN)_6$. This assumption was supported by experiments conducted in several mixed solutions below 100 mmol/L by us and by Lee et al.[5] The concentration distribution near the electrode surface is essential in the simulations; here a digital simulation method based on finite difference approximations was used to obtain the concentration distribution in potential cycling experiments,[20−22] and the concrete diffusion equations have been described elsewhere.[20−22] The simulation programs written in VB 5.0 have been carefully checked, and they gave results that agree with electrochemical theories related to potential cycling and step modulations.[21] Diffusion coefficients as follows were used for simulating experimental data, i.e., $D_o = 7.65 \times 10^{-6}$ cm^2/s for $K_3Fe(CN)_6$ and $D_R = 6.5 \times 10^{-6}$ cm^2/s for $K_4Fe(CN)_6$.[22,23] Only the diffusion processes of $K_3Fe(CN)_6$ and $K_4Fe(CN)_6$ were considered in the simulation.

RESULTS AND DISCUSSION

Electrochemical Processes of Cobalt Complexes with Ethylenediamine (en) and 1,10-Phenanthroline (phen) in 0.5 mol/L Na_2SO_4 Aqueous Solutions. As shown in Figures 2 and 3, simultaneous responses of current, ΔR_1, Δf_s, and ΔL_1 to potential cycling were all reversible with potential for 60.0 mmol/L $CoSO_4$ aqueous solutions containing 0.4 mol/L en + 0.5 mol/L Na_2SO_4 and 50.0 mmol/L $CoSO_4$ aqueous solutions containing 0.2 mol/L phen + 0.5 mol/L Na_2SO_4, respectively. Increases of R_1 and L_1 as well as decreases of f_s were observed after electrochemical oxidation of the cobalt(II)−en solution; however, decreases of R_1 and L_1 as well as increases of f_s were found after oxidation of the cobalt(II)−phen solution. As listed in Table 1, absolute values of responses of ΔR_1 and Δf_s in potential step experiments from −0.8 to −0.2 V vs SCE were positively related to the concentration of $CoSO_4$ added into the solutions. Values of ΔR_1, Δf_s, and ΔL_1 were very minor in both potential cycling and step experiments between −0.8 and −0.2 V vs SCE for 0.4 mol/L en + 0.5 mol/L Na_2SO_4 aqueous solution ($\Delta R_1 < \pm 0.1$ Ω, $\Delta f_s < \pm 4$ Hz). We also conducted potential cycling experiments between −0.2 and 0.5 V vs SCE in 50.0 mmol/L $FeSO_4$ aqueous solution containing 0.2 mol/L phen + 0.5 mol/L Na_2SO_4 (experimentally the Fe−phen complexes were not electroactive in this potential region), but much smaller changes in ΔR_1, Δf_s, and ΔL_1 than those shown in Figure 3 were found ($\Delta R_1 < \pm 0.1$ Ω, $\Delta f_s < \pm 3$ Hz). In

Table 1. Responses of ΔR_1 and Δf_s of a 9-MHz EQCIS after the Potential Step from −0.8 to −0.2 V vs SCE for $CoSO_4$ Aqueous Solutions Containing 0.4 mol/L Ethylenediamine + 0.5 mol/L Na_2SO_4

C_{CoSO_4} (mmol L^{-1})	ΔR_1 (Ω)	Δf_s (Hz)	$\Delta R_1/\Delta f_s$ (Ω Hz^{-1})
10.0	0.4	−6.3	−0.064
30.0	0.8	−10.7	−0.075
60.0	1.8	−21.3	−0.085
90.0	2.7	−31.1	−0.087

(20) Feldberg, S. W. In *Electroanalytical Chemistry*; Bard, A. J., Ed.; Marcel Dekker: New York, 1969; Vol. 8.
(21) Bard, A. J.; Faulkner, L. R. *Electrochemical Methods: Fundamentals and Applications*; John Wiley & Sons: New York, 1980.
(22) Xie, Q.; Wei, W.; Nie, L.; Yao. S. *Anal. Chem.* **1993**, *65*, 1888.
(23) Adams, R. N. *Electrochemistry at Solid Electrodes*; Marcel Dekker: New York, 1969; Chapter 8.

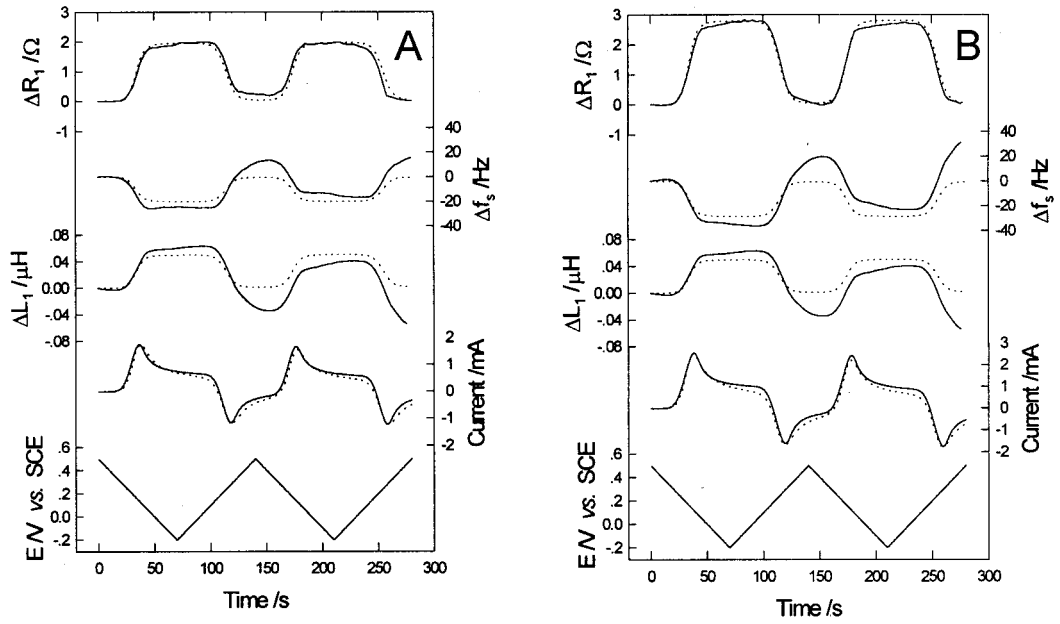

Figure 4. Simultaneous responses of current, ΔR_1, Δf_s, and ΔL_1 to potential cycling for a 9-MHz crystal in 60.0 (A) and 90.0 mmol/L (B) $K_3Fe(CN)_6$ aqueous solutions containing 1.0 mol/L KCl, respectively. dE/dt = 10 mV/s. Solid lines, experimental; dashed lines, simulated by using eqs 1−4, $E^{\circ\prime}$ = 0.220 V vs SCE, k_s = 0.000 51 cm/s, α = 0.54, D_o = 7.65 $\times 10^{-6}$ cm^2/s, and D_R = 6.5 $\times 10^{-6}$ cm^2/s.

addition, an experiment under conditions shown in Figure 3 but only by decreasing the concentration of phen to 0.15 mol/L gave responses for ΔR_1, Δf_s, and ΔL_1 almost identical to those shown in Figure 3. These findings may indicate that electrochemical oxidation of the reduced species and reduction of the oxidized species were the main causes for responses of ΔR_1, Δf_s, and ΔL_1, and the electrical double-layer effects or effects of electrosorption of ions and possible adsorption of phen on the responses were minor and might be neglected for the systems shown in Figures 2 and 3. However, such effects must be considered at relatively small concentrations of electroactive species because of the weak depletion layer effect. In addition, values of Δf_{sL} and ΔL_L calculated from eq 8 by assuming $\Delta R_L = \Delta R_1$ are close to the experimental ones, as shown in Figures 2 and 3. The relationships between dynamic responses of ΔR_1 and Δf_s in the potential cycling experiments are $\Delta R_1 = -0.0861\Delta f_s + 0.103$ ($r = 0.9830$) for the cobalt−en system and $\Delta R_1 = -0.0892\Delta f_s - 0.0776$ ($r = 0.9783$) for the cobalt−phen system, respectively, and relative deviations of the slopes from the value of −0.0986 Ω/Hz calculated from eq 8 are only 13 and 10%, respectively. Moreover, values of $\Delta R_1/\Delta f_s$ for the cobalt(II)−en solutions at 60 and 90 mmol/L concentrations in potential step experiments from −0.8 to −0.2 V vs SCE deviated from the calculated value of −0.0986 Ω/Hz only by 14 and 12%, respectively, as listed in Table 1, although for the 10 and 30 mmol/L cobalt(II)−en solutions the deviations were larger, which is possibly ascribed to the influences of the electrical double-layer effects and the electrosorption of ions. It should be noted that a roughly equivalent deviation was reported by Calvo et al. in a nonelectrochemical experiment to examine effects of solution density and viscosity on ΔR_1 and Δf_s by using a series of sucrose aqueous solutions.[15] They obtained a slope of f_s vs R_1 of −10.66 Hz/Ω, which is also slightly larger than the calculated value of −9.45 Hz/Ω for their crystal (13% deviation).[15] Their result was in good agreement with the data reported previously by Zhou et al. for sucrose aqueous solutions of similar concentration.[24] In our opinion, in addition to possible influences of adsorption of ions or molecules and the electrical double-layer effects, the roughness of the electrode surface may also contribute to the small differences between the calculated and experimental values of ΔR_1, Δf_s, ΔL_1 and the slope of ΔR_1 vs Δf_s, since Martin's model needs a very smooth surface.[9,11] In fact, the influence of the electrode roughness on the oscillating frequency of EQCM had been noticed by Schumacher et al.[8] Therefore, it seems reasonable to assume that responses of equivalent circuit parameters here that roughly satisfy eq 9 resulted predominantly from local variations of solution density and viscosity during the electrode reactions, i.e., local changes in liquid loading inside the depletion layer.

Electrochemical Processes of $K_3Fe(CN)_6$ and $K_4Fe(CN)_6$ Aqueous Solutions Containing 1.0 mol/L KCl. Simultaneous responses of current, ΔR_1, Δf_s, and ΔL_1 to potential cycling between 0.5 and −0.2 V for 60.0 and 90.0 mmol/L $K_3Fe(CN)_6$ aqueous solutions containing 1.0 mol/L KCl are shown in Figure 4, and those for 90.0 mmol/L $K_4Fe(CN)_6$ aqueous solution containing 1.0 mol/L KCl are shown in Figure 5. It is seen that R_1 changed reversibly with potential and ΔR_1 coincided well with the result from digital simulation with use of eqs 2 and 4, demonstrating the correctness of eq 2 even in spatially nonuniform solutions. Therefore, one may quantify the local change in $(\rho_L\eta_L)^{1/2}$ near the electrode surface using eq 2 and the ΔR_1 response of the EQCIS here, as shown in Figure 6 for 90.0 mmol/L $K_3Fe(CN)_6$ aqueous solution containing 1.0 mol/L KCl. It is seen that the calculated values of changes in $(\rho_L\eta_L)^{1/2}$ from eq 2 are in good agreement with the simulated ones from the independently determined values of ρ_L and η_L given in eq 4, indicating that the ΔR_1 response can be well used for evaluating local changes in liquid loading inside the depletion layer. It should be noted that the maximum local viscosity−density effect obtained from the

(24) Zhou, T.; Nie, L.; Yao, S. *J. Electroanal. Chem.* **1990**, *293*, 1.

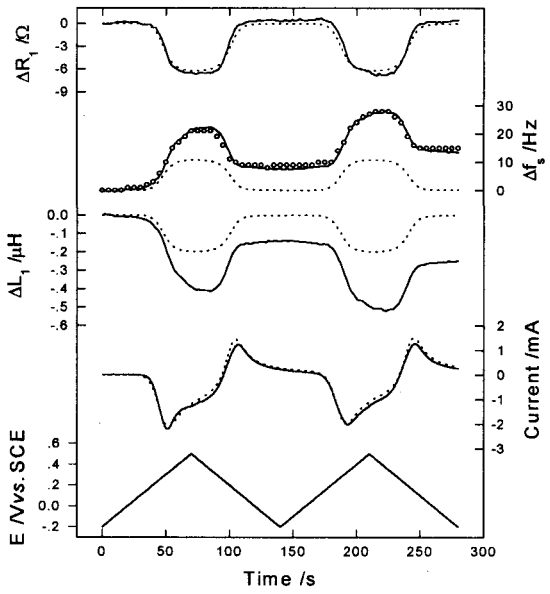

Figure 5. Simultaneous responses of current, ΔR_1, Δf_s, and ΔL_1 to potential cycling for a 5-MHz crystal in 90.0 mmol/L $K_4Fe(CN)_6$ aqueous solution containing 1.0 mol/L KCl. Open circles shows oscillating frequency obtained from an EQCM of the same crystal in the same solution. Other conditions are the same as those in Figure 4.

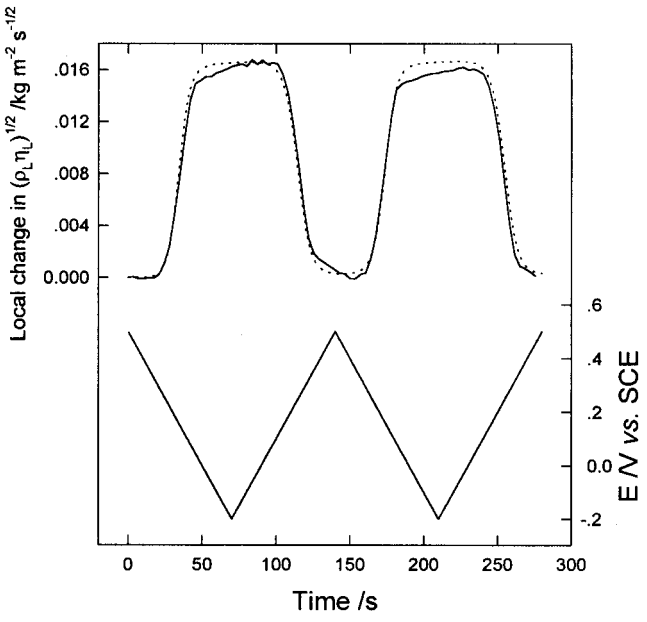

Figure 6. Time dependence of local changes in $(\rho_L\eta_L)^{1/2}$ near the electrode surface in the experiment shown in Figure 4B. Solid line, calculated according to eq 2 and the experimental response of ΔR_1 shown in Figure 4B; dashed line, simulated by using eq 4 and the electrochemical parameters taken in Figure 4B.

simulation was 0.016 57 kg m^{-2} $s^{-1/2}$, which is greater than the difference of the value of $(\rho_L\eta_L)^{1/2}$ of 90.0 mmol/L $K_4Fe(CN)_6$ from that of 90.0 mmol/L $K_3Fe(CN)_6$ estimated from eq 4, 0.014 68 kg m^{-2} $s^{-1/2}$. This phenomenon can be explained by the fact that the diffusion of $K_4Fe(CN)_6$ is slower than that of $K_3Fe(CN)_6$ ($D_R = 6.5 \times 10^{-6}$ cm^2/s and $D_o = 7.65 \times 10^{-6}$ cm^2/s), and thus, during the reduction of $K_3Fe(CN)_6$, the departure of the electrogenerated $K_4Fe(CN)_6$ from the electrode surface via its diffusion should also be slower than its generation via the reduction of $K_3Fe(CN)_6$, leading to a local concentration of $K_4Fe(CN)_6$ greater than 90 mmol/L near the electrode surface.[20−22] In fact, if $D_o = D_R = 6.5 \times 10^{-6}$ cm^2/s was assumed, we obtained from the simulation a maximum local viscosity−density effect of 0.014 51 kg m^{-2} $s^{-1/2}$, which is very close to the difference of the value of $(\rho_L\eta_L)^{1/2}$ of 90.0 mmol/L $K_4Fe(CN)_6$ from that of 90.0 mmol/L $K_3Fe(CN)_6$ calculated from eq 4. Moreover, if $D_o = 6.5 \times 10^{-6}$ cm^2/s and $D_R = 7.65 \times 10^{-6}$ cm^2/s were assumed in the simulation, a maximum local viscosity−density effect of 0.012 32 kg m^{-2} $s^{-1/2}$ was obtained. These results demonstrate that the diffusion coefficients taken can influence the simulation, and thus the difference between the diffusion coefficients of the reduced and oxidized species should be considered for a precise simulation of the depletion layer effect.

However, unlike the cobalt−en and cobalt−phen systems mentioned above, drifts of Δf_s and ΔL_1 were found here at oxidation potentials. The rising drifts of frequency and the decreasing drifts of motional inductance could be observed cycle by cycle even for 50 potential cycles, without significant decreases in drifting amplitudes of Δf_s and ΔL_1. Potential scan rate from 5 to 20 mV/s had negligible effects on values of ΔR_1, but a slower scan rate resulted in more significant drifts of Δf_s and ΔL_1. As shown in Figure 5, it is seen for a 5-MHz crystal that drifting phenomena were also found in responses of Δf_s, ΔL_1, and the oscillating frequency recorded by using a conventional EQCM with an oscillating circuit similar to that reported previously.[1] The oscillating frequency responses of the EQCM were very close to the frequency response of the EQCIS. The drifting amplitude of Δf_s was some 0.3 times of that found by a 9-MHz EQCIS for the same solution, which coincides well with the ratio of the mass sensitivity of a 5-MHz crystal to that of a 9-MHz one, 0.31, according to the Sauebrey equation.[2] To the best of our knowledge, generally changes in liquid properties, viscosity properties of foreign films on the electrode, mass loading on the electrode surface, and electrode surface stress are able to cause frequency shifts at a fixed temperature. Here variations of solution density and viscosity near the electrode surface, or variations of viscosity properties of foreign films (if exist), should be reversible with potential, as indicated by the simultaneously observed changes in motional resistance, and significant changes in electrode surface stress are also not expected. Therefore, we assign the drifts of Δf_s and ΔL_1 as a mass effect. Accordingly, one may easily separate the frequency and inductance responses to mass changes from the total responses, simply by subtracting the calculated values of Δf_{sL} and ΔL_L according to eq 8 with the assumption of $\Delta R_L = \Delta R_1$ from responses of Δf_s and ΔL_1. For instance, for 90.0 mmol/L $K_4Fe(CN)_6$ aqueous solution containing 1.0 mol/L KCl as shown in Figure 5, one potential cycle caused ~45 ng loss of the electrode mass.

The mechanism responsible for the drifts of Δf_s and ΔL_1 is very interesting, and a lot of time were consumed in elucidating the possible mechanism. Considering that the cycle-by-cycle drifting phenomena of frequency and motional inductance observed in long time potential cycling experiments are very difficult to be reasonably explained by the possibility of the formation of a Prussian blue film and/or a persistent monolayer of $Fe(CN)_6^{3-/4-}$ reported previously,[25,26] we finally concluded that cyanide and chloride corrosion of the gold electrode at oxidation potentials

(25) Feldman, B. J.; Melroy, O. R. *J. Electroanal. Chem.* **1987**, *234*, 213.

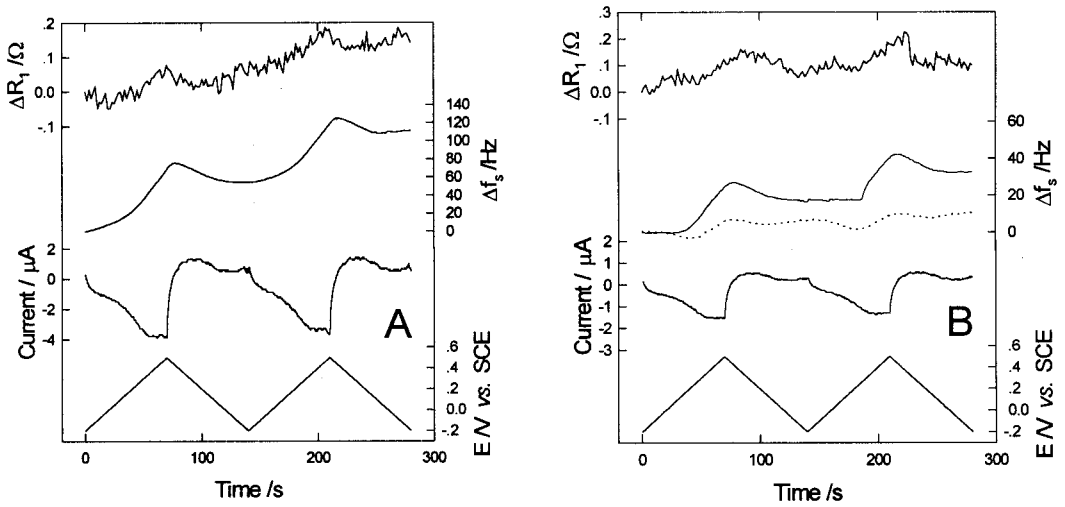

Figure 7. Simultaneous responses of current, ΔR_1 and Δf_s to potential cycling for a 9-MHz crystal in 1.0 mol/L KCl aqueous solutions containing 9.0×10^{-5} (A) and 9.0×10^{-6} (B) mol/L KCN, respectively. dE/dt = 10 mV/s. Dashed line in Figure 7B shows Δf_s response for 1.0 mol/L KCl aqueous solution containing 9.0×10^{-7} mol/L KCN.

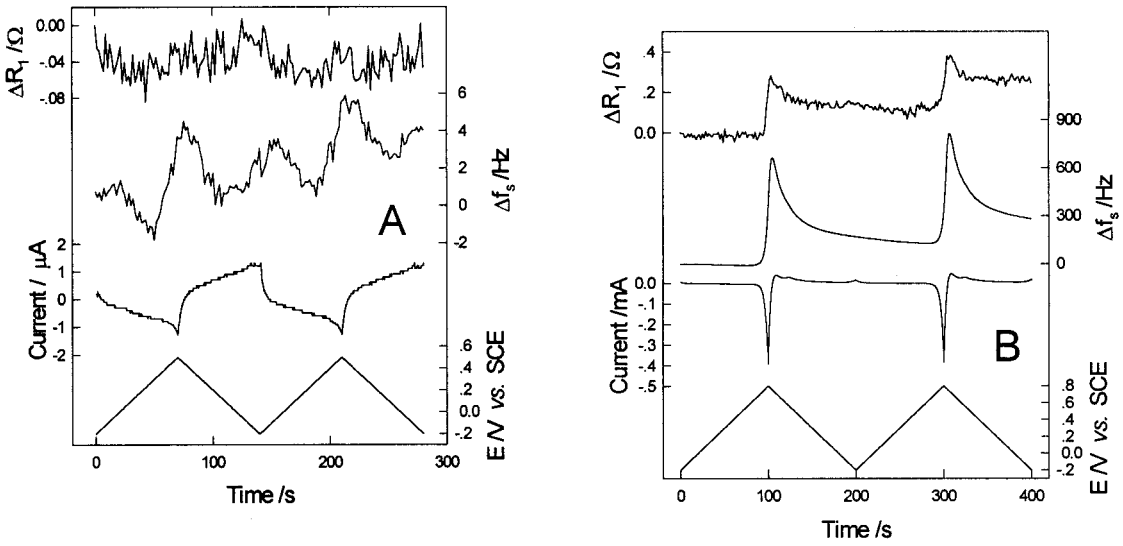

Figure 8. Simultaneous responses of current, ΔR_1, and Δf_s to potential cycling between −0.2 and +0.5 V (A) and between −0.2 and +0.8 V (B) for a 9-MHz crystal in 1.0 mol/L KCl aqueous solution. dE/dt = 10 mV/s.

may play an important role in the drifting phenomena of Δf_s and ΔL_1 observed here, based on the following experiments and considerations:

(1) By using the complex stability constants (10^{42} for $Fe(CN)_6^{3-}$ and 10^{35} for $Fe(CN)_6^{4-}$),[27,28] one may simply find that the concentration of CN^- being freed from 90 mmol/L $Fe(CN)_6^{3-}$ is 9.16×10^{-7} mol/L and that from 90 mmol/L $Fe(CN)_6^{4-}$ is 9.16×10^{-6} mol/L. If considering a corrosion mechanism as follows

$$Au = Au^+ (c)$$

$$Au^+ (c) + 2CN^- (9.16 \times 10^{-7}\ mol/L) = Au(CN)_2^- (x) \quad (10)$$

we obtain

$$10^{38.3} = \frac{C_{Au(CN)_2^-}}{C_{Au^+} C_{CN^-}^2} = \frac{x}{c(9.16 \times 10^{-7})^2} \quad (11)$$

where $10^{38.3}$ is the complex stability constant of $Au(CN)_2^-$.[27,28]

By assuming a concentration of Au^+ as $c = 1.66 \times 10^{-24}$ mol/L (one gold ion per liter), the equilibrium concentration of $Au(CN)_2^-$, x, is as high as 278 mol/L, indicating an obvious shift of reaction 10 toward the formation of soluble $Au(CN)_2^-$. These calculations indicate that dissolution of gold to form soluble complexes of gold with cyanide in 90 mmol/L $Fe(CN)_6^{4-}$ or $Fe(CN)_6^{3-}$ aqueous solution is thermodynamically favorable. Kinetically, dissolution of gold at oxidation potentials may benefit from the electrostatic affinities between a positively charged gold surface and cyanide or $Fe(CN)_6^{3-/4-}$ anions and thus easier formation of soluble

(26) Smalley, J. E.; Geng, L.; Feldberg, S. W.; Rogers, L. C.; Leddy, J. *J. Electroanal. Chem.* **1993**, *356*, 181.

(27) Dean, J. A. Lange's *Handbook of Chemistry*, 12th ed.; Dean, J. A., Ed.; McGraw-Hill: New York, 1979; pp 5−54.

(28) Yin, Y. J. *Handbook of University Chemistry*; Shangdong Science and Technology Press: Jinan, China, 1985.

complexes of gold with cyanide, since values of PZC of gold are generally negative to 0 V vs SCE.[29]

(2) Drifting phenomena of Δf_s were found in 1.0 mol/L KCl aqueous solutions containing KCN (KCN is highly poisonous; treat with great care), as shown in Figure 7. The drift values of f_s observed in 1.0 mol/L KCl aqueous solutions containing 9.0×10^{-6} mol/L KCN and containing 9.0×10^{-7} mol/L KCN are roughly comparable with those found in $K_3Fe(CN)_6$ and $K_4Fe(CN)_6$ aqueous solutions containing 1.0 mol/L KCl, as shown in Figures 4 and 5.

(3) A slight drifting phenomenon of Δf_s, which may be ascribed to gold dissolution, was observed at potentials positive to ~0.4 V vs SCE in 1.0 mol/L KCl blank aqueous solution, as shown in Figure 8A. This slight dissolution of gold may assist the further dissolution of gold via cyanide as fresh gold, which is highly active, should be produced on some surface sites, and this seems to be the cause for the rising drift phenomena of frequency in 1.0 mol/L KCl electrolyte that we observed, but Lee et al. did not observe similar phenomena in Na_2SO_4.[5] As shown in Figure 8B, the potential at which the gold electrode is significantly dissolved was ~0.69 V vs SCE in 1.0 mol/L KCl, which is in good agreement with ~0.7 V vs SCE reported in a previous study on the electrochemical oxidation of gold in 0.6 mol/L NaCl solution.[30] The mass per mole electron (MPE) values, which were calculated from the mass sensitivity value, frequency shift values, and electric charges in range I (from 0.69 to 0.8 to 0.75 V), range II (from 0.75 to 0.6 V), and range III (from 0.6 to 0.4 V) were 67.1, 71.3, and 65.7 g/mol·e, respectively. These MPE values are roughly $^1/_3$ of the molar mass of gold, indicating an identical $3e^-$ dissolution process of gold to that suggested by an EQCM study conducted in a $HClO_4$ solution containing chloride ions.[31] The changes in motional resistance shown in Figure 8B may result mainly from increases in solution density and viscosity near the electrode surface due to the formation of soluble $AuCl_4^-$. Since the observed ΔR_1 values are still small even for very significant dissolution of gold here, relatively slight dissolution of gold in ferrocyanide and ferricyanide solutions will cause negligible changes in R_1; therefore, values agreeable with the simulated ones could be obtained, as shown in Figures 4 and 5. This finding also implies that the ΔR_1 response can be well used for evaluating local changes in liquid loading inside the depletion layer compared with responses of Δf_s and ΔL_1.

CONCLUSION

The electrochemical quartz crystal impedance system has been used for the first time to investigate depletion layer effects on equivalent circuit parameters in electrochemical processes of $CoSO_4$ aqueous solutions containing 0.4 mol/L en + 0.5 mol/L Na_2SO_4, 0.2 mol/L phen + 0.5 mol/L Na_2SO_4 and $K_3Fe(CN)_6$, or $K_4Fe(CN)_6$ aqueous solutions containing 1.0 mol/L KCl, respectively. The former two systems gave results in fair agreement with eq 9, indicating almost net depletion layer effects. However, drifts of Δf_s and ΔL_1 were found at oxidation potentials for the latter two systems, besides their reversible changes with potential. The drifts observed in the latter two systems are believed to result from changes in electrode mass, and cyanide and chloride corrosion of gold electrode at oxidation potentials may play an important role for the drifting phenomena. It is concluded that quantitative analyses of changes in motional resistance, series resonant frequency, and motional inductance obtained from EQCIS on the basis of eqs 8 and 9 provide the possibility for differentiating the net depletion layer effect in an electrochemical process from changes in the electrode mass. In addition, the response of ΔR_1 rather than responses of Δf_s and ΔL_1 can be well used for evaluating local changes in liquid loading inside the depletion layer.

ACKNOWLEDGMENT

This work was supported by the National Natural Science Foundation of China, the Science and Technology Foundation of Hunan Province for Youth as well as the Educational Committee Foundations of China and Hunan Province.

Received for review December 16, 1998. Accepted July 31, 1999.

AC981390Z

(29) Dobos, D. *Electrochemical Data*; Elsevier: Amsterdam, 1975.
(30) Ling, Y.; Elkenbracht, J. C.; Flanagan, W. F.; Lichter, B. D. *J. Electrochem. Soc.* **1997**, *144*, 2689.
(31) Ye, S.; Ishibashi, C.; Shimazu, K.; Uosaki, K. *J. Electrochem. Soc.* **1998**, *145*, 1614.